A 3000 K laboratory emission spectrum of water

Pierre-François Coheur
Service de Chimie Quantique et Photophysique, Université Libre de Bruxelles, 50 Av. F.D. Roosevelt, B-1050 Bruxelles, Belgium

Peter F. Bernath
Department of Chemistry, University of Waterloo, Waterloo, Ontario N2L 3G1, Canada and Department of Chemistry, University of Arizona, Tucson, Arizona 85721

Michel Carleer and Reginald Colin
Service de Chimie Quantique et Photophysique, Université Libre de Bruxelles, 50 Av. F.D. Roosevelt, B-1050 Bruxelles, Belgium

Oleg L. Polyansky[a)]
Sektion Spektran und Strukturdokumentation, University of Ulm, Helmholtzstraasse 22, D-89069 Ulm, Germany

Nikolai F. Zobov and Sergei V. Shirin
Institute of Applied Physics, Russian Academy of Science, Uljanov Street 46, Nizhnii Novgorod, 603950 Russia and Department of Physics and Astronomy, University College London, London WC1E 6BT, United Kingdom

Robert J. Barber and Jonathan Tennyson[b)]
Department of Physics and Astronomy, University College London, London WC1E 6BT, United Kingdom

(Received 15 October 2004; accepted 19 November 2004; published online 7 February 2005)

An emission spectrum of hot water with a temperature of about 3000 K is obtained using an oxy-acetylene torch. This spectrum contains a very large number of transitions. The spectrum, along with previous cooler laboratory emission spectra and an absorption spectrum recorded from a sunspot, is analyzed in the 500–2000 cm^{-1} region. Use of a calculated variational linelist for water allows significant progress to be made on assigning transitions involving highly excited vibrational and rotational states. In particular emission from rotationally excited states up to $J=42$ and vibrational levels with up to eight quanta of bending motion are assigned. © *2005 American Institute of Physics*. [DOI: 10.1063/1.1847571]

I. INTRODUCTION

Vibration-rotation bands of hot water vapor are prominent in the spectra of flames and cool stars.[1] As early as the 1890s these "steam bands" were recorded from the infrared emission obtained during the combustion of hydrocarbons.[2] They can also be seen in rocket plumes and in jet engine exhausts.[1] Absorption of hot water vapor appears in the near infrared spectra of M-type stars[3] and brown dwarfs.[4]

In the laboratory, the first modern data for hot water vapor were recorded by workers[5,6] at Meudon Observatory near Paris using an oxygen-hydrogen torch with a temperature of about 2900 K. The water emission in the 2800–9000 cm^{-1} spectral region was recorded with a high resolution Fourier transform spectrometer. The rotational analysis was carried by the traditional methods of pattern recognition and combination differences. This pioneering effort provided some assignments up to $J=35$, which lies at 11 656 cm^{-1} in the ground vibrational level.

The main difficulty in assigning the hot water spectrum, apart from dealing with an irregular jumble of lines from a light asymmetric top, is the presence of "anomalous centrifugal distortion." As the water molecule rotates, it experiences a substantial geometrical distortion, particularly of the bending angle, from centrifugal forces. The usual Watson rotational Hamiltonian diverges and an excessive number of centrifugal distortion terms need to be retained to fit the experimental data.[7] This divergence of the Hamiltonian limits the utility of predictions of line positions with higher J and, in particular, higher K_a values than those already included in the fit. It is this anomalous centrifugal distortion that limited the range of the rotational assignments in the original torch spectrum—not the signal-to-noise ratio of the spectra.

Various schemes[7–11] have been devised to reformulate the rotational Hamiltonian to improve convergence. These efforts have enjoyed some success, but the most satisfactory approach to assigning the hot water spectrum lies in abandoning perturbation theory altogether. The observation of the very dense water spectrum near 10 μm in a sunspot[12] (Water on the Sun) prompted the application of a variational approach[13] based on solving the full vibration-rotation Schrödinger equation to predict the energy levels with high quality *ab initio* potential surfaces.[14,15] The variational ap-

[a)]Permanent address: Institute of Applied Physics, Russian Academy of Science, Uljanov Street 46, Nizhnii Novgorod 603950, Russia.
[b)]Electronic mail: j.tennyson@ucl.ac.uk

proach has yielded the majority of the new assignments and energy levels as tabulated by Tennyson *et al.*[16]

Highly excited levels of water can also be obtained through the analysis of overtone spectra. In contrast to the spectra obtained with furnaces and torches, the overtone data are rotationally cold. Overtone spectra have allowed the assignment of vibrational levels with up to eight quanta of OH stretching (at 25 120 cm^{-1}) to be observed.[17] Highly excited bending levels, which are expected to show interesting effects,[18,19] are not detected by overtone spectroscopy. The highest pure bending level that is reliably assigned[16] is (060), although tentative assignments of some levels up to (0 10 0) has been made on the basis of perturbations.[20]

Very recently another source of highly excited energy levels of water has been developed by Coudert *et al.*[21] Coudert *et al.* have fitted the rotational energy levels obtained mainly from a far infrared emission spectrum of water vapor excited by a radio frequency discharge. The lines associated with the first eight vibrational levels were fitted with the theoretical approach of Coudert.[11] Very few new levels were seen, but the accuracy of the levels was significantly improved.

The goal of the current research is to obtain a new spectrum of a torch over a wider spectral range and then apply the variational approach to extend the assignments of the water levels to higher J, K_a levels. In addition, the torch spectrum allows us to assign different vibrational levels, particularly new pure bending levels.

The temperature of the water vapor in an oxy-acetylene or oxy-hydrogen torch can reach 3000 K, but the line width is about 0.05–0.10 cm^{-1} because of pressure broadening at 1 atm. The pressure can be reduced, but this also reduces the signal-to-noise ratio. The torch unfortunately has extensive emission from extraneous molecules such as CO, CO_2, and OH, in addition to water. Furnace sources allow the spectrum of pure water vapor to be recorded, but then the temperature is limited to a maximum of about 2000 K by the softening of the ceramic walls of the confining tube. Carbon tube furnaces can also reach 3000 K but the water gas reaction,

$$H_2O(g) + C(s) \rightarrow CO(g) + H_2(g),$$

prevents their use as a source of hot water emission. Despite its limitations, the oxy-acetylene torch at atmospheric pressure was used for all of the work reported in this paper. As shown below this approach yields a considerable amount of information.

II. EXPERIMENTAL PROCEDURE

Hot water vapor was produced in an oxy-acetylene torch at atmospheric pressure. Emission spectra of the flame were recorded using a Bruker IFS 120 M Fourier transform spectrometer between 500 and 13000 cm^{-1}, using a variety of combinations of filters and detectors. For the 500–2000 cm^{-1} region investigated here, two different settings were used: KBr entrance window and beam splitter were used to record the spectra in the lower wave number region, along with a HgCdTe detector. With this setup, the entrance aperture was 4 mm in diameter and the spectral resolution was 0.03 cm^{-1} (30 cm maximum optical path difference, mopd). A CaF_2 window and beam splitter were used to enhance the signal-to-noise ratio above 1900 cm^{-1}, where an InSb detector was used. In that spectral region, a 2 mm aperture was chosen and the spectral resolution was set to 0.05 cm^{-1} (18 cm mopd). In both regions 512 scans were co-added, thereby producing emission spectra with very low noise, see Fig. 1.

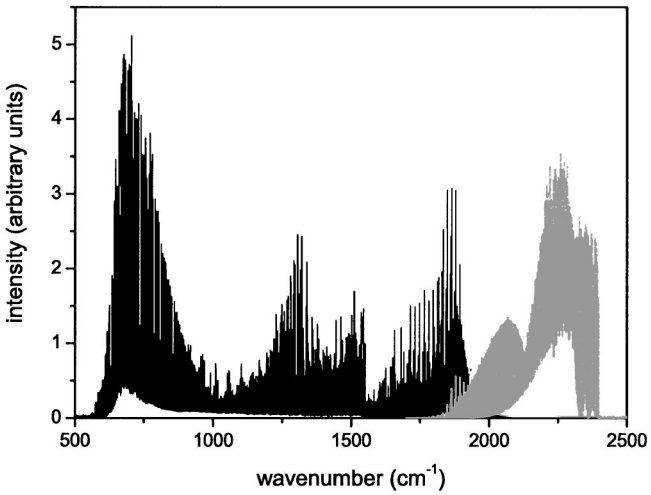

FIG. 1. Raw emission spectrum of the oxy-acetylene flame in the 500–2500 cm^{-1} spectral region.

The line positions and intensities in the spectra have been determined using the WSPECTRA program.[22] In order to get rid of some weak ringing, the lines were first identified in spectra that were apodized using a Norton–Beer weak function. The fits were then performed on the unapodized spectra using the sinc instrument line shape function to determine line positions and intensities, see Fig. 2. In the fitting procedure a Voigt molecular line shape function was used, and both Gaussian and Lorentzian contributions were fitted. The WSPECTRA program also automatically fitted the baseline. It is worth pointing out that the spectra have not been corrected for the response of the optics and the detectors. The relative

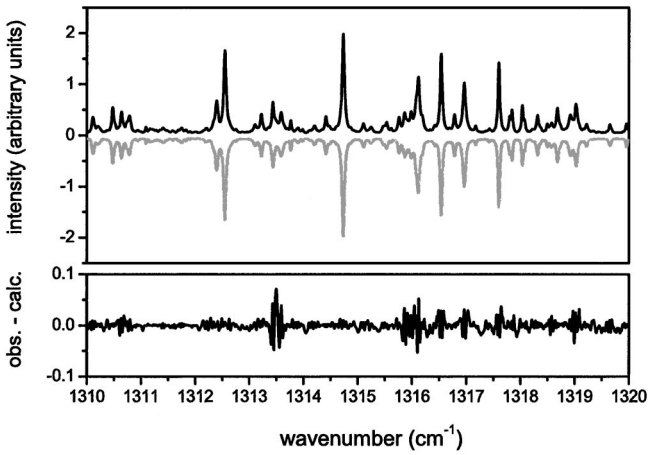

FIG. 2. Example of a WSPECTRA fit of our data. The black line and gray line are, respectively, the observed and the calculated spectrum, with the residuals below on an expanded scale.

line intensities are therefore not reliable over large spectral ranges and should be used with care.

The wave number calibration was performed using the laboratory hot water vapor measurements of Tereszchuk *et al.*[23] in the 4880–7550 cm^{-1} region, which is not presented in this paper. The consistency of the calibration was verified using the CO line positions in the 1-0 band, as archived by the National Institute of Standard and Technology.[24] Our measurements agree with the NIST data to within 5×10^{-3} cm^{-1}, which is satisfactory considering the fact that the CO pressure-induced wave number shifts were not taken into account in the comparison. The value of 5×10^{-3} cm^{-1} is taken as a "worst-case" estimate of the absolute accuracy of our measurements. A statistical uncertainty originating from the quality of the spectral fit also has to be taken into account for each line. This statistical uncertainty is of the order of 10^{-4} cm^{-1} for strong and well-defined lines, but reaches significantly larger values for the numerous weak or blended lines.

As is obvious from Figs. 1 and 2, the spectra are very dense over the entire wave number region investigated, showing in addition to water lines, emission features of CO, CO_2, and OH. The OH lines were identified in the spectra by comparing the calibrated list of measured line positions between 5000 and 13000 cm^{-1} to calculated values, obtained using the spectroscopic data of Colin *et al.*[25] and Melen *et al.*[26] Vibrational levels up to $v=8$ were considered in the comparison, and the very weak satellite lines were neglected. CO lines were similarly identified by using the HITEMP database[27] as a reference, with $v=8$ as the highest vibrational level, and both the ^{12}CO and ^{13}CO isotopes were considered. Observed CO lines are due to rotational transitions in the $v=0$ and 1 vibrational levels, with only five lines in the $v=2$ vibrational level.

A search for CO_2 lines was made using data taken from the carbon dioxide spectroscopic database (CDSD) system of the Institute of Atmospheric Optics of the Siberian Branch of the Russian Academy of Sciences.[28] This database contains transitions from HITRAN, HITEMP, and GEISA databases and can be used to simulate spectra at different temperatures, pressures, optical path lengths, and line shape parameters. It transpires that the CO_2 lines at 3000 K in the 500–2000 cm^{-1} region are approximately three orders of magnitude weaker than the OH lines in this region. This means that contrary to our expectations, CO_2 lines are barely detectable in the spectrum analyzed in this paper. Indeed the only transitions identified lie below the cutoff used for measuring lines. The strong vibrational spectrum of CO_2 starts at about 2200 cm^{-1} and will be taken into account in our future analysis of water molecule in the stretching mode region. In the region of interest in the current paper, out of the 10 100 measured lines, 363 were assigned to CO and 141 were assigned to pure rotational transitions of OH.

III. THEORETICAL ANALYSIS

Spectra of hot water vapor in the 500–2000 cm^{-1} region considered in this paper have been recorded in the laboratory (pure rotational spectrum $T=1800$ K, 373–934 cm^{-1} region, and v_2 band spectrum $T=1800$ K, 933–2500 cm^{-1} region) in emission and in sunspots ($T\approx3200$ K, 722–1011 cm^{-1} region) in absorption.[12,29,30] It was decided to analyze the current data along side these older spectra. Figure 3 compares a portion of these spectra.

The laboratory emission spectra from heated cells were recorded at a lower temperature than the present spectrum, so are less suitable for searching for highly excited transitions of water. Indeed the previous v_2 band spectrum contains some 40% fewer lines than the oxy-acetylene torch spectrum. However in the 373–934 cm^{-1} region, the older emission spectrum has about 1000 more lines than the torch spectrum. The higher pressure in the torch spectrum means that many weak lines are obscured by stronger ones. The sunspot spectrum contains more than three times the number of lines, in absorption, than the present emission spectrum over the region in which they overlap. The sunspot spectrum thus remains the richest in terms of hidden information or number of lines per wave number. The main drawback of the sunspot spectrum is its limited wave number range due to absorptions in the Earth's atmosphere. Many of our assigned lines lie outside the range of the sunspot spectrum. Furthermore, the high density of the lines, up to 50 per wave number, requires very precise frequency predictions from theoretical calculations when dealing with the weaker lines. Almost all the strong and medium absorption lines were assigned in our previous work,[13,30] but few of the weaker lines.

These hot water spectra contain information on highly excited vibrational and rotational levels. To be explicit, we report below emission arising from levels with up to eight quanta of bending excitation and levels rotationally excited to $J=42$. Our theoretical model therefore must be capable of dealing with this high degree of excitation.

In analyzing the spectra we used a calculated variational linelist for hot water. The BT1 linelist was constructed explicitly to provide reliable models for the opacity of water in the atmosphere of cool stars. It therefore considered all levels of the molecule with $J\leqslant50$ and lying up to 30 000 cm^{-1} above the $J=0$ ground state. The linelist used the recent, spectroscopically determined potential energy surface of Shirin *et al.*[31] and special care was taken to ensure complete convergence of these levels as this has proved to be a problem with previous hot water linelists (see Ref. 30). Full details of this linelist, including a database containing all 620×10^6 transition intensities will be presented elsewhere.[32]

The first step in analyzing the torch spectrum, after marking the OH and CO lines, was to make trivial assignments, that is, assignments made using our hot water linelist and previously known experimental energy levels of the water molecule.[16] As the observed linewidths are relatively large a significant number (about 20%) of the experimental lines have double (or even triple) trivial assignments. In fact the number of multiply assigned lines was even higher after making our initial trivial assignments. In this initial analysis we used the theoretical linelist with an intensity cutoff about half that of the weakest experimental lines and did not compare theoretical and experimental intensities. In making our

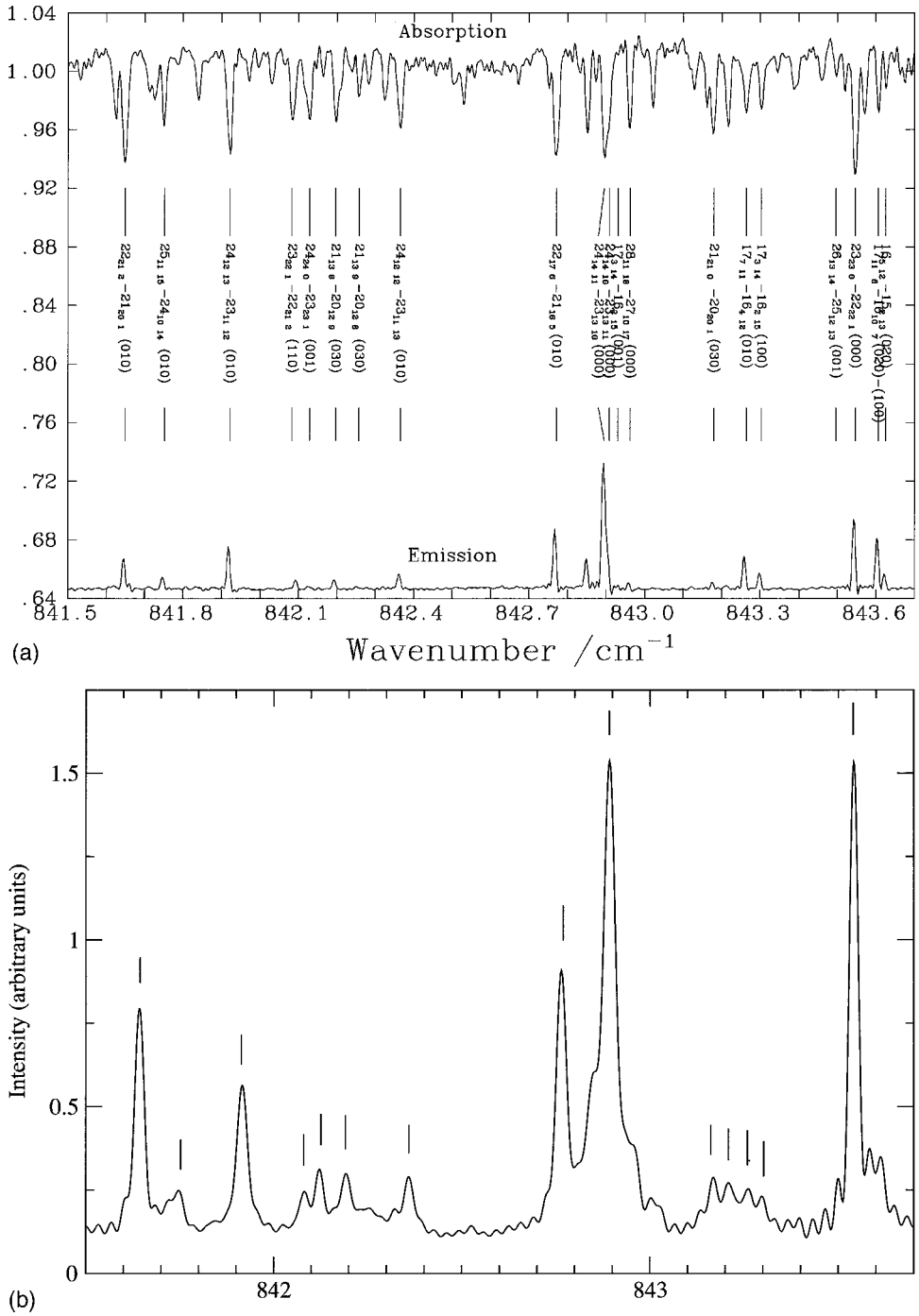

FIG. 3. Upper panel: sunspot absorption (upper trace) and laboratory emission from heated cell spectra (lower trace) from work (Ref. 30) near 840 cm^{-1}. Lower panel: torch spectrum in the same region; vertical lines denote assigned transitions.

final trivial assignments we retained only lines which give at least 20% of the total line intensity. About 80% of the measured lines were assigned trivially.

In analyzing the remaining unassigned lines in the torch spectrum we employed different methods for different unknown levels. These levels can be roughly divided into three groups: (a) highest J, low K_a rotational levels in the lowest vibrational levels (000), (010), and (020); (b) high $J(=20-30)$, intermediate and high K_a, low vibrational levels (000), (010), (020), (030), and (040); and (c) high bending levels (050), (060), (070), and (080).

For assigning transitions involving the highest J and low K_a rotational levels we used the method of branches, which has been described elsewhere.[30,33] To predict the energy of an unknown level we used not only the calculated value, but also looked at the difference between observed and calculated values for the same branch of levels with lower J values. The BT1 linelist is based on a spectroscopically determined potential energy surface for which only levels with $J=0$, 2, and 5 were used in the fit. The standard deviation for that fit was 0.1 cm^{-1}, but for the highest J levels known previously the typical observed minus calculated (obs−calc)

value grows to 0.8 cm^{-1} for (000) state, 0.4 cm^{-1} for (010) and 0.3 cm^{-1} for (020). Although these errors are much larger than the average spacing between measured lines, the differences increase smoothly with J. This means we can predict the positions of unknown higher J levels with an accuracy of about 0.02 cm^{-1}. This is sufficient for unambiguous assignments.

Some of the lines linking levels with the highest J values were found only in the laboratory pure rotational spectra,[30] as they are obscured by stronger neighboring lines in the higher linewidth torch spectra. We were unable to assign these levels previously due to the lack of sufficiently accurate predictions from variational calculations. The present analysis allowed us to determine about 100 different levels and increase the maximum J value from 35 to 42 (from 11656 to 16406 cm^{-1}) for the ground vibrational level, from 32 to 39 for (010), and from 31 to 36 for (020). The newly determined highest J, low K_a rotational levels for the (000), (010), and (020) vibrational levels are presented in Table I.

The majority of the assigned levels belong to states with high $J(=20-30)$, intermediate or high K_a, and low bending vibrational excitation. Within a set of levels with a given J and vibrational state the obs−calc changes smoothly with changing values of K_a and K_c. This means one can predict unknown levels with an accuracy sufficient for assignments. Our previous work on hot water spectra gave us enough known levels for each set to make this method of assignment possible. Our energy levels are given in the EPAPS archive.[34]

Most of the determined levels in the two groups mentioned above were obtained from a single pure rotational transition, as in each case this line is the strongest for the given level. It should be noted that the corresponding vibration-rotation transitions are largely not present in the torch spectrum since such transitions involving levels with high K_a are too weak to be seen.

The fitting procedure employed to obtain the spectroscopically determined potential[31] used experimental energy levels for bending states up to (060). For levels belonging to the (040), (050), and (060) vibrational levels the residuals of the fit were small and changed smoothly with quantum numbers. Assignments could therefore be made using theoretical predictions. Most levels determined were confirmed by combination differences, making them reliable. About 20 levels of the (070) bending level have been previously determined from overtone spectroscopy,[20,35] along with the 6_{34} level of the (080) vibrational level.[20] As these levels were not used in fitting, the residuals for them grows to 0.5 cm^{-1} for (070) and 1 cm^{-1} for (080). This is due to the bending vibrational levels approaching the barrier to linearity. Furthermore, for these states the obs−calc depends significantly on the value of K_a but has almost no dependence on J for a given K_a. This allowed us to assign 17 additional levels in (070) and 9 in (080). The assignments to (070) can be considered as reliable, especially those confirmed by combination differences. The assignments involving (080) are more tentative. The assigned rotational levels in the (060), (070), and (080) vibrational levels are presented in Table II.

For the (070) and (080) bending levels no transitions

TABLE I. Wave numbers of the assigned highest J rotational levels in (000), (010), and (020) vibrational levels in cm^{-1}.

J	K_a	K_c	Level	E
36	0	36	000	12 290.5959
36	1	36	000	12 290.5959
36	1	35	000	12 921.2711
36	2	35	000	12 921.2711
36	2	34	000	13 433.3356
36	3	34	000	13 433.3356
36	3	33	000	13 935.4309
36	4	33	000	13 935.4309
36	20	17	000	19 398.9036
36	20	16	000	19 398.9036
36	21	16	000	19 750.1982
36	21	15	000	19 750.1982
36	22	15	000	20 101.7967
36	22	14	000	20 101.7967
36	23	14	000	20 452.4935
36	23	13	000	20 452.4935
37	0	37	000	12 940.1441
37	1	37	000	12 940.1441
37	1	36	000	13 585.9949
37	2	36	000	13 585.9949
37	2	35	000	14 099.7715
37	3	35	000	14 099.7715
37	3	34	000	14 614.1750
37	4	34	000	14 614.1750
37	24	14	000	21 553.1329
37	24	13	000	21 553.1329
38	0	38	000	13 604.4879
38	1	38	000	13 604.4879
38	1	37	000	14 265.3170
38	2	37	000	14 265.3170
38	2	36	000	14 778.6740
38	3	36	000	14 778.6740
38	3	35	000	15 305.9609
38	4	35	000	15 305.9609
39	0	39	000	14 283.4348
39	1	39	000	14 283.4348
39	1	38	000	14 959.0419
39	2	38	000	14 959.0419
39	2	37	000	15 469.7102
39	3	37	000	15 469.7102
39	3	36	000	16 010.5323
39	4	36	000	16 010.5323
40	0	40	000	14 976.7975
40	1	40	000	14 976.7975
40	1	39	000	15 666.9690
40	2	39	000	15 666.9690
40	2	38	000	16 172.5357
40	3	38	000	16 172.5357
41	0	41	000	15 684.3814
41	1	41	000	15 684.3814
41	1	40	000	16 388.8934
41	2	40	000	16 388.8934
42	0	42	000	16 406.0561
42	1	42	000	16 406.0561
33	0	33	010	11 953.6676
33	1	33	010	11 953.6676
33	1	32	010	12 640.1170
33	2	32	010	12 640.1170

TABLE I. (*Continued.*)

J	K_a	K_c	Level	E
33	2	31	010	13 115.9905
33	3	31	010	13 115.9905
33	3	30	010	13 639.8400
33	4	29	010	14 085.0896
33	7	26	010	15 228.6773
33	15	18	010	17 420.0613
33	16	17	010	17 778.7798
33	17	16	010	18 130.4003
33	18	15	010	18 492.5424
33	20	13	010	19 211.6078
33	21	13	010	19 581.1881
33	21	12	010	19 581.1881
33	22	12	010	19 939.7786
33	22	11	010	19 939.7786
33	24	10	010	20 645.8124
33	24	9	010	20 645.8124
34	0	34	010	12 557.4625
34	1	34	010	12 557.4625
34	1	33	010	13 264.2962
34	2	33	010	13 264.2962
35	0	35	010	13 177.6869
35	1	35	010	13 177.6869
35	1	34	010	13 904.3971
35	2	34	010	13 904.3971
36	0	36	010	13 814.3780
36	1	36	010	13 814.3780
36	1	35	010	14 560.2728
36	2	35	010	14 560.2728
37	0	37	010	14 467.5545
37	1	37	010	14 467.5545
37	1	36	010	15 231.8067
37	2	36	010	15 231.8067
37	2	35	010	15 653.8554
37	3	35	010	15 653.8554
38	0	38	010	15 137.1779
38	1	38	010	15 137.1779
39	0	39	010	15 823.2561
39	1	39	010	15 823.2561
32	0	32	020	12 913.3436
32	1	32	020	12 913.3436
33	0	33	020	13 511.4038
33	1	33	020	13 511.4038
34	0	34	020	14 128.3021
34	1	34	020	14 128.3021
35	0	35	020	14 763.9356
35	1	35	020	14 763.9356
36	0	36	020	15 418.0188
36	1	36	020	15 418.0188

have been observed to the 0_{00} rotational level. However it is possible to obtain an estimate for the vibrational band origin for these two levels by looking at the systematic differences between the observed and calculated rotational term values. Table III presents estimates for these band origins and a summary of the energy levels determined in this work. A complete tabulation of these levels is given in the EPAPS archive.[34]

The many trivial assignments made in this work can be

TABLE II. Wave numbers for rotational term values in the (060), (070), and (080) vibrational levels in cm^{-1}.

J	K_a	K_c	Level	E
0	0	0	060	8 869.9538
1	1	1	060	8 998.0996
1	1	0	060	9 004.6170
2	2	1	060	9 271.2847
3	1	2	060	9 139.0734
3	2	1	060	9 344.3799
3	3	0	060	9 628.7737
4	2	3	060	9 438.2526[a]
4	3	2	060	9 725.7365
4	4	1	060	10 049.2800
5	0	5	060	9 210.1607
5	1	4	060	9 377.2237
5	2	4	060	9 556.7927[a]
5	2	3	060	9 565.5203
5	3	2	060	9 847.2247
5	4	2	060	10 171.0870
5	4	1	060	10 171.2898
5	5	1	060	10 519.2778[b]
5	5	0	060	10 519.2778[b]
6	1	6	060	9 400.6406
6	1	5	060	9 533.5828
6	2	5	060	9 698.0404[b]
6	2	4	060	9 714.4540
6	3	4	060	9 991.0166
6	3	3	060	9 992.3307
6	4	3	060	10 316.3808
6	5	2	060	10 666.2485
7	0	7	060	9 487.9479
7	1	6	060	9 714.7602
7	3	4	060	10 162.1936
7	4	4	060	10 484.2790
7	4	3	060	10 486.3693[a]
7	5	2	060	10 837.7072
7	6	2	060	11 199.7595
7	6	1	060	11 199.7370
7	7	1	060	11 564.2145
7	7	0	060	11 564.2145
8	1	8	060	9 697.2256
8	2	7	060	10 047.3069[a]
8	3	6	060	10 348.1658
8	3	5	060	10 356.0418[b]
8	4	5	060	10 672.4910
8	4	4	060	10 678.8623[b]
8	5	4	060	11 032.0251
8	5	3	060	11 032.4511[a]
8	6	3	060	11 395.4898
8	6	2	060	11 394.9593
8	8	1	060	12 263.3487
9	1	8	060	10 143.6997
9	2	8	060	10 254.3984
9	3	7	060	10 558.6984[b]
9	3	6	060	10 574.3192
9	4	5	060	10 894.2476[b]
9	6	4	060	11 612.7597
9	6	3	060	11 613.0694[b]

TABLE II. (*Continued.*)

J	K_a	K_c	Level	E
10	1	10	060	10 069.0056[a]
10	2	9	060	10 483.2868
10	3	8	060	10 785.3000
10	4	7	060	11 143.4201[a]
10	6	5	060	11 853.8368
10	8	3	060	12 720.4711
10	8	2	060	12 720.4944
11	0	11	060	10 259.4551
11	1	11	060	10 283.9173[a]
11	1	10	060	10 656.5089
11	2	9	060	10 826.3404[b]
11	3	8	060	11 084.3958[b]
11	4	7	060	11 392.2185[b]
11	5	6	060	11 755.8094[b]
12	1	12	060	10 518.0698
12	1	11	060	10 942.1613[b]
12	2	11	060	11 003.6709[a]
12	2	10	060	11 112.0853[b]
12	3	10	060	11 326.8032[a]
12	4	9	060	11 676.3099[b]
12	5	8	060	12 038.3255[b]
13	0	13	060	10 756.2885
13	1	13	060	10 773.1396[b]
13	1	12	060	11 246.8263[a]
13	2	11	060	11 411.2944[b]
13	3	10	060	11 690.6398[a]
13	5	8	060	12 356.5256
14	0	14	060	11 036.1947[b]
14	1	14	060	11 043.9614
14	2	13	060	11 607.5558[a]
15	0	15	060	11 330.4470[b]
16	0	16	060	11 654.8647[b]
16	1	16	060	11 658.8880[a]
17	0	17	060	12 004.1736[b]
1	1	1	070	10 334.3666
1	1	0	070	10 341.0547
2	1	2	070	10 374.8919
2	2	1	070	10 703.3386[a]
3	0	3	070	10 224.5606[b]
3	1	3	070	10 435.5297
3	1	2	070	10 475.6581
3	2	1	070	10 775.3009
3	3	0	070	11 136.7986[b]
4	1	4	070	10 516.1570
4	1	3	070	10 582.9251
4	2	3	070	10 871.3547[a]
4	3	2	070	11 233.8187[b]
5	1	5	070	10 616.7746
5	1	4	070	10 716.5816[a]
5	2	4	070	10 990.9667
5	2	3	070	10 990.1665[b]
6	1	6	070	10 737.4070
6	1	5	070	10 875.8198
6	2	5	070	11 134.1762
6	3	4	070	11 496.9058[b]
7	1	7	070	10 878.1735

TABLE II. (*Continued.*)

J	K_a	K_c	Level	E
7	1	6	070	11 060.8235
7	2	6	070	11 300.7657[b]
7	3	5	070	11 660.8681
7	3	4	070	11 666.9403
8	0	8	070	10 897.3083[b]
8	1	8	070	11 039.2005
8	1	7	070	11 270.5126[a]
8	2	7	070	11 490.4559[a]
8	2	6	070	11 482.0729
9	1	9	070	11 221.7144
9	1	8	070	11 504.7708[b]
9	2	7	070	11 689.3420
10	1	10	070	11 424.9390[a]
10	2	9	070	11 938.9806[a]
10	3	8	070	12 302.1714[b]
11	0	11	070	11 573.2541[b]
11	1	10	070	12 043.1979[a]
11	4	7	070	13 778.6454
12	0	12	070	11 779.5362
12	2	11	070	12 479.7768[b]
13	0	13	070	1 2064.1500
2	2	1	080	12 148.2928[b]
3	0	3	080	11 390.5763[b]
3	1	2	080	11 813.6815[b]
4	1	4	080	11 851.5431[b]
6	2	5	080	12 585.1205[b]
7	1	6	080	12 417.0858[a]
9	1	8	080	12 880.4466[a]
10	1	10	080	12 769.9046[a]
10	2	9	080	13 416.0819[b]
11	1	10	080	13 443.8321[b]

[a]The levels confirmed by combination differences.
[b]The levels obtained from one transition.

used to gauge the accuracy with which any energy levels are determined. For strong lines the trivial assignments agree with the line position with a typical error of 0.003 cm^{-1}. This error is thus appropriate for the high J, intermediate or high K_a, and low bending vibrational excitation levels assigned here. For weaker transitions this level of agreement drops and the high J levels and high bending levels are probably only accurate to about 0.01 cm^{-1}.

TABLE III. Summary of rotational energy levels for each vibrational level. Experimental origins (Ref. 16), number of new levels N and maximum J value.

Level	E	N	J
000	0.000	179	42
010	1 594.746	149	39
020	3 151.630	75	36
030	4 666.790	14	22
040	6 134.015	24	21
050	7 542.437	58	20
060	8 869.954	37	17
070	10 085.9(2)	17	12
080	11 253.8(5)	9	11

The EPAPS archive also contains a listing of the three spectra of hot water (re)analyzed here: the oxy-acetylene torch spectrum obtained with $T=3000$ K for the 529–2000 cm^{-1} region, the pure rotational laboratory emission spectrum $T=1800$ K, 373–934 cm^{-1} region, and the sunspot absorption spectrum $T\approx3200$ K, 722–1011 cm^{-1} region.[12,29,30] After completing work on the torch spectrum we performed a trivial assignment of the sunspot spectrum and then checked for consistency between theoretical and experimental intensities. Incorrect trivial assignments, those for which the theoretical line was too weak for a relatively strong experimental line, were removed. Even with OH and SiO lines marked, about half of measured lines in the sunspot spectrum remain unassigned. Assignments obtained from the torch spectrum have also been added to the pure rotational laboratory spectrum.

IV. CONCLUSIONS

In this paper we report the observation of a new spectrum obtained from an oxy-acetylene torch with a temperature of about 3000 K. This spectrum is rich in emission from hot water and, in principle, contains a significant quantity of information.

More accurate and more extensive variational linelist has been used to analyze the torch spectrum with different strategies employed for transitions involving three different types of highly excited states. Altogether about 85% of the 10 100 lines measured in the torch spectrum in the 500–2000 cm^{-1} range have been assigned. The majority of the remaining unassigned lines lie in pure rotational transition region (500–1000 cm^{-1}). These lines belong mostly to high J rotational transitions within vibrational states with stretching excitation. Some of these lines could, in principle, be assigned now. However a more productive strategy is to analyze these transitions at the same time as the 2000–5000 cm^{-1} region, which contains the stretching vibration-rotation transitions. This approach will give combination differences to confirm the assignments made.

The bending region (1000–2000 cm^{-1}) contains further information on the higher bending states. To make progress on these highly excited bending states will require an improved fit to the potential energy surface to give more reliable predictions. One method is to include iteratively the determined energy levels of the high-lying bending states to give better predictions and hence more levels. This method has recently been used to analyze successfully the emission spectrum of hot (1800 K) D_2O.[36]

ACKNOWLEDGMENTS

Financial support provided by the Fonds National de la Recherche Scientifique (FNRS, Belgium, FRFC Convention No. 2.4536.01) and the "Actions de Recherches Concertees" (Communaute Francaise de Belgique) is acknowledged. This work was also supported by The Royal Society, INTAS, the UK Engineering and Physical Science Research Council, the NASA astrophysics program, the Canadian Natural Sciences and Engineering Council, and the Russian Fund for Fundamental Studies.

[1] P. F. Bernath, Phys. Chem. Chem. Phys. **4**, 1501 (2002).
[2] A. G. Gaydon, *The Spectroscopy of Flames*, 2nd ed. (Chapman and Hall, London, 1974).
[3] S. K. Leggett, F. Allard, C. Dahn, P. H. Hauschildt, T. H. Kerr, and J. Rayner, Astrophys. J. **535**, 965 (2000).
[4] J. D. Kirkpatrick, I. N. Reid, J. Liebert *et al.*, Astrophys. J. **519**, 802 (1999).
[5] J.-M. Flaud, C. Camy-Peyret, and J.-P. Maillard, Mol. Phys. **32**, 499 (1976).
[6] C. Camy-Peyret, J.-M. Flaud, J.-P. Maillard, and G. Guelachvili, Mol. Phys. **33**, 1641 (1977).
[7] O. L. Polyansky, J. Mol. Spectrosc. **112**, 79 (1985).
[8] V. I. Starikov and S. N. Mikhailenko, J. Phys. B **33**, 2141 (2000).
[9] P. Chen, J. C. Pearson, H. M. Pickett, S. Matsuura, and G. A. Blake, Astrophys. J., Suppl. Ser. **128**, 371 (2000).
[10] V. G. Tyuterev, J. Mol. Spectrosc. **151**, 97 (1992).
[11] R. Lanquetin, L. H. Coudert, and C. Camy-Peyret, J. Mol. Spectrosc. **206**, 83 (2001).
[12] L. Wallace, P. Bernath, W. Livingston, K. Hinkle, J. Busler, B. Guo, and K.-Q. Zhang, Science **268**, 1155 (1995).
[13] O. L. Polyansky, N. F. Zobov, S. Viti, J. Tennyson, P. F. Bernath, and L. Wallace, Science **277**, 346 (1997).
[14] H. Partridge and D. W. Schwenke, J. Chem. Phys. **106**, 4618 (1997).
[15] O. L. Polyansky, A. G. Csaszar, S. V. Shirin, N. V. Zobov, P. Bartletta, J. Tennyson, D. W. Schwenke, and P. J. Knowles, Science **299**, 539 (2003).
[16] J. Tennyson, N. F. Zobov, R. Williamson, O. L. Polyansky, and P. F. Bernath, J. Phys. Chem. Ref. Data **30**, 735 (2001).
[17] N. F. Zobov, D. Belmiloud, O. L. Polyansky *et al.*, J. Chem. Phys. **113**, 1546 (2000).
[18] J. P. Rose and M. E. Kellman, J. Chem. Phys. **105**, 7348 (1996).
[19] M. S. Child, T. Weston, and J. Tennyson, Mol. Phys. **96**, 371 (1999).
[20] A. Bykov, O. Naumenko, L. Sinitsa, B. Voronin, J.-M. Flaud, C. Camy-Peyret, and R. Lanquetin, J. Mol. Spectrosc. **205**, 1 (2001).
[21] L. H. Coudert, O. Pirali, M. Vervloet, R. Lanquetin, and C. Camy-Peyret, J. Mol. Spectrosc. **228**, 471 (2004).
[22] M. Carleer, in *Remote Sensing of Clouds and Atmosphere*, edited by J. E. Russell, K. Schafer, and O. Lado-Bardowski (SPIE, Washington, 2001), Vol. 5, pp. 337–342.
[23] K. Tereszchuk, P. F. Bernath, N. F. Zobov, S. V. Shirin, O. L. Polyansky, N. I. Libeskind, J. Tennyson, and L. Wallace, Astrophys. J. **577**, 496 (2002).
[24] A. G. Maki and J. S. Wells, http://physics.nist.gov/PhysRefData/wavenum/html/contents.html
[25] R. Colin, P.-F. Coheur, M. Kiseleva, A. C. Vandaele, and P. F. Bernath, J. Mol. Spectrosc. **214**, 225 (2002).
[26] F. Melen, A. J. Sauval, N. Grevesse, C. B. Farmer, Ch. Servais, L. Delbouille, and G. Roland, J. Mol. Spectrosc. **174**, 490 (1995).
[27] L. S. Rothman, C. Camy-Peyret, J.-M. Flaud *et al.* (private communication).
[28] See http://spectra.iao.ru
[29] N. F. Zobov, O. L. Polyansky, J. Tennyson, J. A. Lotoski, P. Colarusso, K.-Q. Zhang, and P. F. Bernath, J. Mol. Spectrosc. **193**, 118 (1999).
[30] O. L. Polyansky, N. F. Zobov, S. Viti, J. Tennyson, P. F. Bernath, and L. Wallace, J. Mol. Spectrosc. **186**, 422 (1997).
[31] S. V. Shirin, O. L. Polyansky, N. F. Zobov, P. Barletta, and J. Tennyson, J. Chem. Phys. **118**, 2124 (2003).
[32] R. J. Barber and J. Tennyson (unpublished).
[33] O. L. Polyansky, N. F. Zobov, S. Viti, J. Tennyson, P. F. Bernath, and L. Wallace, Astrophys. J. **489**, L205 (1997).
[34] See EPAPS Document No. E-JCPSA6-122-010506 for electronic versions of all the torch spectrum between 500 and 2000 cm^{-1}, plus assignments, as well the 373–933 cm^{-1} laboratory spectrum and the 722–1011 cm^{-1} sunspot spectrum with updated assignments. Newly determined energy levels for vibrational states $(0v_20)$ with $v_2=0-8$ are also given. A direct link to this document may be found in the online article's HTML reference section. The document may also be reached via the EPAPS homepage (http://www.aip.org/pubservs/epaps.html) or from ftp.aip.org in the directory /epaps/. See the EPAPS homepage for more information.
[35] O. Naumenko and A. Campargue, J. Mol. Spectrosc. **221**, 221 (2003).
[36] S. V. Shirin, N. F. Zobov, O. L. Polyansky, J. Tennyson, T. Parekunnel, and P. F. Bernath, J. Chem. Phys. **120**, 206 (2004).